Paper No. 253--50

Measurement and Some Discussions on Dynamic* Load Sharing in Planetary Gears

Teru HAYASHI**, Yuan Xie Li+, Iwao HAYASHI***
Kinichi ENDOU++ and Wataru WATANABE+++

The biggest problem in use of the planetary gears is uneven load sharing of every planet gear. For solving the problem, many new designs have been offered, but there is not an exact method to confirm their results. Applying the principle that the shearing strain on the beam is constant in one side of the loaded point, a new measurement method of detecting the shearing strains on the planet gear axes is offered. The measurement by the method is done on actual planetary gears using the power circulation type test rig. As a result it is made clear that the offered measuring method of the load sharing in the planetary gears is practically useful and that the dynamic load sharing condition in actual planetary gears is considerably different from the estimated one from the static condition.

Key Words : Gear, Planetary Gear, Load, Load Sharing, Measurement

1. Introduction

In general, the load sharing of each planet gear in the planetary gears is unequal because of the manufacturing errors of the parts and the assembling errors of them. This is the hardest problem in putting the planetary gears to practical use and many analyses and experiments have been done and many kinds of designs have been tried to overcome the problem. However, there is not yet any reliable method to confirm their effects. Necessarily, the indirect methods have been used in which the strains on the side or outer surfaces of the internal gear ring at the points where the planet gears pass at the same time are measured or the strains of internal gear or sun gear at the roots of the teeth with which the planet gears mesh at the same time are measured. The authors had tried some kinds of methods with direct measurement of the loads on planet gear axes but did not succeed. For example, the method with the measurement of the bending strains on planet gear axes is simple but can not be used in general case when the positions of loads shift on the axes.

This time, assuming that the shearing stress at the fixed end of a planet gears is not affected by the position of the load, a method with measurement of the shearing strains on planet gear axes is tested and experimental measurement are done using actual planetary gears.

2. Principle of the Measuring Method

An outline of the planet gear axis of solid and cantilever type is shown in Fig.1(a). There, when the load P is applied to the point separated by l from the strain measuring points A, B, C and D, the shearing force Q(=P) and the bending moment M(=P·x) at the section of the point which is distant X from the loaded point become as shown in Fig.(b) and (c) respectively and the shearing stress distribution due to Q on the surface of the section at the measuring point becomes as shown in Fig.(d). As the bending stress σ_b becomes 0 and the shearing stress becomes maximum value τ_{max} (=4 · P/(3 · A), where, A : the sectional area of the axis) at the points C and D which are on the neutral plane, the load P can be obtained without knowing the position of the loaded

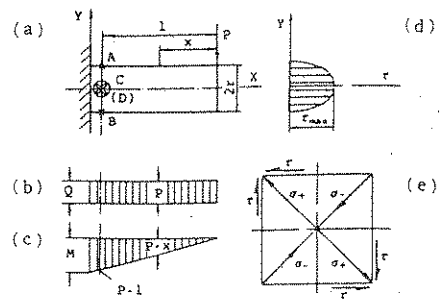

Fig.1 Relation between load and shear strain

* Recieved 6th June, 1984
** Professor, Research Laboratory of Precision Machinery and Electronics, Tokyo Institute of Technology (4259 Nagatsuta, Midori-ku, Yokohama, JAPAN). 227)
*** Associate Professor, same as the above affiliation.
+ Research Fellow, Changchun Institute of Optics and Fine Mechanics, Academia Sinica, (Gong nong Guang chang, Chang chun, CHINA).
++ Toyoseimituzoki Co., (3-11-4 Owada-cho Hachioji-shi, JAPAN 192).
+++ Matsushita Electric Industry Co., (2-7 Matsuba-cho, Kadoma-shi, Osaka, JAPAN 571).

point and using the measured values of the shearing strain at the points. Using the rossete type strain gauges to measure the τ_{max} value, the stress σ at the point in the direction of the gauge length becomes τ_{max} and the measured strain ε becomes as follows,

$$\varepsilon=\frac{\sigma}{E}=\frac{\tau_{max}}{E}=\frac{4}{3}\cdot\frac{P}{AE} \quad \cdots\cdots\cdots\cdots(1)$$

(Under the experimental condition of P=1000N, E=21x10^4 N/mm^2 and A=314mm^2, we get $\varepsilon=20\times10^{-6}$)

If two sets of rossete type strain gauges at the points C and D are used as the circuit of 4 elements bridges the measured value will be increased to 4 times the above value ($\varepsilon=80\times10^{-6}$ full scale).

3. The Analyses of Measurement Errors

In the measurement of the errors caused by the following reasons are expected. They are (1) a linear deviation of the measuring point and (2) a directional deviation of the load due to the additional centrifugal load to the transmitting load. These effects on the measurement errors will be discussed in the following.

3.1 The general equations on measured value

When the rossete type strain gauges that are shown in Fig.2(a) are put at the point distant a from the neutral plane and

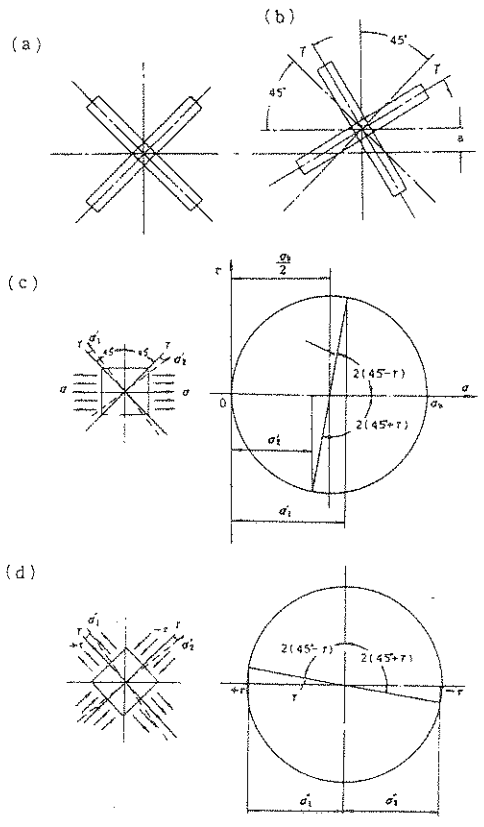

Fig.2 Error due to allignment of strain gage and Mohr's stress circle

their directions are inclined γ° to the normal directions (45° against the axis), as shown in Fig.(b), the tensile stresses σ_1' and σ_2' which occur in the strain gauges due to the bending stress component σ_b and σ_1'' and σ_2'' due to the shearing stress component τ are obtained by the aid of Mohle's Stress Circles as follows (see Fig.(c) and (d)).

$$\sigma_1'=\frac{\sigma_b}{2}(1+\sin 2\gamma) \qquad \sigma_1''=\tau\cos 2\gamma$$

$$\sigma_2'=\frac{\sigma_b}{2}(1-\sin 2\gamma) \qquad \sigma_2''=-\tau\cos 2\gamma$$

When both of the stresses σ_b and τ are present, the stresses on respective gauges σ_1 and σ_2 are as follows,

$$\sigma_1=\sigma_1'+\sigma_1''=\frac{\sigma_b}{2}(1+\sin 2\gamma)+\tau\cos 2\gamma$$

$$\sigma_2=\sigma_2'+\sigma_2''=\frac{\sigma_b}{2}(1-\sin 2\gamma)-\tau\cos 2\gamma .$$

Then, the strains ε_1 and ε_2 due to σ_1 and σ_2 respectively are as follows,

$$\varepsilon_1=\frac{\sigma_1}{E}, \quad \varepsilon_2=\frac{\sigma_2}{E}$$

The voltage V detected by the strain gauges is as follows. There, two rossete type strain gauges are located at symmetrical points to the axis and near the fixed end of a planet gear axis as shown in Fig.1(a).

$$V=k\cdot 2(\varepsilon_1-\varepsilon_2)$$

$$=K(\sigma_b\sin 2\gamma+2\tau\cos 2\gamma) \quad \cdots\cdots\cdots\cdots(2)$$

where,

$$\tau=\frac{4}{3\pi r^2}\left\{1-\left(\frac{a}{r}\right)^2\right\}^{1/2}\cdot P ,$$

$$\sigma_b=\frac{a}{r}\cdot\frac{4l}{\pi r^3}\cdot P ,$$

K : constant,

r : radius of the beam section.

The load P', that is detected when the positional error a and the angular error γ exist, is determined from Eq.(2) as follows,

$$\frac{P'}{P}=\left[\left\{1-\left(\frac{a}{r}\right)^2\right\}^{1/2}\cos 2\gamma+\frac{3al}{2r^2}\sin 2\gamma\right] \quad \cdots\cdots\cdots\cdots(3)$$

where, P is the value when $a=0$ and $\gamma=0$. Considering $a/r\ll 1$ and $\gamma\ll 1$, the higher order terms of (a/r) can be neglected, and we have

$$\frac{P'}{P}=1-\left\{\frac{1}{2}\left(\frac{a}{r}\right)+2\gamma^2-3\frac{l}{r}\left(\frac{a}{r}\right)\gamma\right\}$$

or putting $P'=P+\Delta P$, we have

$$\frac{\Delta P}{P}=-\left\{\frac{1}{2}\left(\frac{a}{r}\right)+2\gamma^2-3\frac{l}{r}\left(\frac{a}{r}\right)\gamma\right\} \quad \cdots\cdots\cdots\cdots(4)$$

3.2 The effects of the positional error a and the angular error γ of positioning of the strain gauges

(1) The effect of the positional error a is obtained by putting $\gamma=0$ in Fig.(4), and we have

$$\frac{\Delta P}{P}=-\frac{1}{2}\left(\frac{a}{r}\right)^2 \quad \cdots\cdots(5)$$

(2) The effect of the angular error γ is obtained by putting $a=0$ in Eq.(4), and we have

$$\frac{\Delta P}{P}=-2\gamma^2 \quad \cdots\cdots(6)$$

When the positional error a, the angular error γ or both errors exist when putting the strain gauges on the axis, the error ratios occurring in the measured result ($\Delta P/P$) are numerically obtained using Eq.s (5),(6) and (4), as shown in Table 1.

The experimental values of the error ratios when $\gamma=15^\circ$ are shown in Table 2 and the values almost coincide with (slightly less than) the theoretical values in Table 1. If the errors a and γ are kept less than 1mm and 5° respectively in the experiment the measurement error ratio will be less than 0.8% and they could be neglected for practical use.

3.3 The effect of the deviation θ of the loaded direction :

Considering the centrifugal force on a planet gear, the direction of loading form a planet gear to the planet axis is shifted by θ against the tangential direction of its orbital motion (see Fig.3). In that case, the measured load and the measurement error ratio are obtained by putting $\gamma=0$ and $a=r\sin\theta$ into Eqs.(3) and (4) respectively and they become as follows,

$$\frac{P'}{P}=\cos\theta \quad ,\text{or} \quad \frac{\Delta P}{P}=1-\cos\theta \quad \cdots\cdots(7)$$

Experimental and theoretical results when $\theta=15^\circ$ are shown in Table 3. The results nearly agree with each other. When $\theta=90^\circ$, only the transmission load is measured because the measured load P' becomes 0 theoretically. If the load due to the centrifugal force has to be measured, another set of rossete type strain gauges should be added to the position where $\theta=90^\circ$.

Table 1 Measuring error due to allign ment and fixing position of straing gage

a (mm)	ΔP/P (%)
0.5	-0.1
1	-0.5

r (DEG)	ΔP/P (%)
5	-2
10	-6
15	-13

When errors a and r exist in one time (%)	a (mm) \ r (DEG)	5	10
	0.5	-0.4	-2.6
	1	-0.8	+0.5

(l=14 mm)

Table 2 Experimental values at miss-allignment

Load (N)	1300	3600	6200	8600
error (%)	-12	-9	-10	-10

(r 15°, l=14 mm)

Table 3 Measured value $\Delta P/P$ due to inclination of loading direction θ

θ (DEG)	Exprimental value (%)			Calculated value (%)
15	-1.1	-1.04	-1.06	-1.6

4. Fundamental Experiments

Considering the results of the above discussion on measurement errors, the strain gauges were put on flat planes of 5mm width made near the fixed ends of each planet gear axis of the planet carrier and a fundamental experiment to examine the relation between the values of load and the measured strain was done. There, for applying the load to the planet gear a loading ring as shown in Fig.3 was used to make the experimental condition similar to the condition of the actual planetary gears. The first experiment was done using the A type planet axis, in which the

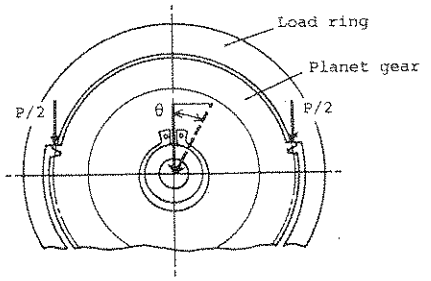

Fig.3 Load ring

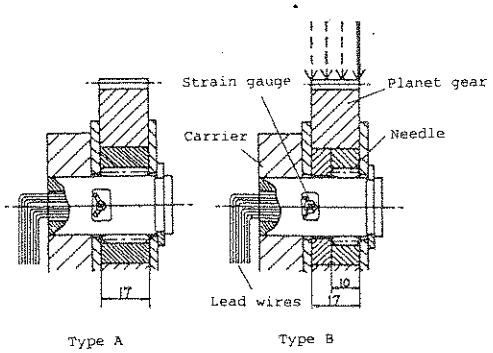

Fig.4 Mechanism of planetary gear bearing (Type A and Type B)

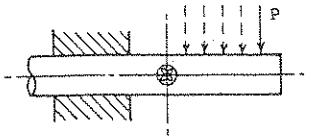

Fig.5 Position of strain gage and Loading position

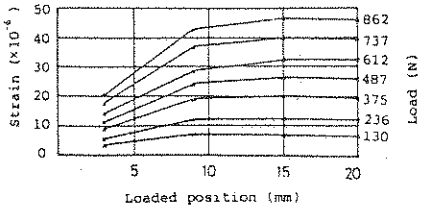

Fig.6 Induced strain of type A bearing as function of loading position

needle bearing had the same width as that of the planet gear as shown in Fig.4, and the strains were measured by changing the loaded position as shown in Fig.5. As a result, the defect that the measured values of the strains changed depending on the axial positions of the loaded points was found out as shown in Fig.6. That is, when the position becomes close (about less than 6mm) to the point where the strain gauges are put the measuring magnification factors are decreased to 50% of the normal. To eliminate the defect, the B type planet axis shown in Fig.4 was used and the result was successful as shown in Fig.7. Thereby the changes of the measuring magnification factors due to the position of the loaded point were very small (less than 2.7% change in maximum). An example of the experimental result about the relation between the load and the measured strain is shown in Fig.8. It is clear from the figure that there is a small difference of less than 6% between the experimental and the theoretical values but repeatability and linearity for practical use of this method are good enough. About the other planet gear axes of the planetary gears, similar relations and a slight differences in the sensitivity are seen. However these differences can be compensated by adjusting the amplifier gain in the instruments.

5. Test Rig and Planetary Gears

5.1 Test rig

The power circulation type test rig as shown in Fig.9 is used for the experiment. The torque is created by twisting the axis S_2. That is, at first, the fixing screws of the coupling in F are released, next, the input gear G_1 is fixed, then, the axis S_2 is twisted with a special spanner (1.2m length) and during the twist the fixing screw is tightened again. The amount of the torque is adjusted reading it from the strain gauge put on the axis S_2. About the mutual effects on the vibration of each planetary gear in the test rig, as the natural frequencies of the high speed axis S_1 and the low speed axis S_2 without the planetary gears connected are 49Hz and 23.5 Hz respectively, the higher frequency components above these frequencies are expected to be insulated.

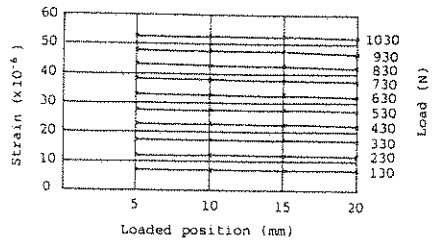

Fig.7 Induced strain of type B bearing as function of loading position

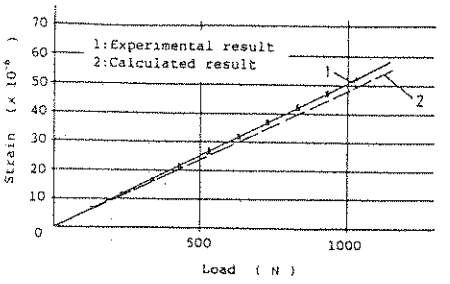

Fig.8 Relation between load and induced strain

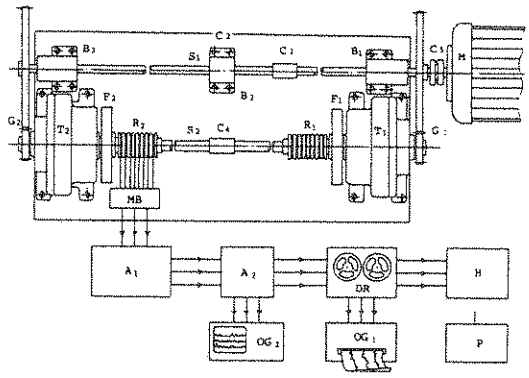

M : Speed varaible induction motor (11kW, 150～2500rpm)
G_1, G_2 : Gears for circulating power (gear ratio $i=3.916$, moment of inertia of gear $J_1=110\,N\cdot mm\cdot s^2$)
B_1, B_2, B_3 : Bearings (roller bearing, two used at each position)
T_1, T_2 : Tested planetary gears (speed increasing and decreasing one)
F_1, F_2 : Flywheel ($J_2=859\,N\cdot mm\cdot s^2$)
S_1 : High speed axle ($k_1=52\times10^6\,N\cdot mm/rad$)
S_2 : Low speed axle ($k_2=94\times10^5\,N\cdot mm/rad$)
C_1～C_4 : Splined shaft coupling (pressed fit)
C_5 : Rubber shaft coupling
R_1, R_2 : Sliprings for measuring strain (8 termainals, made by us)
MB : Matching box
A_1, A_2 : Dynamic strain meter (～10 kHz) DC amplifier (1～10 X)
OG_1 : Electromagnetic oscillograpgh (～2 kHz)
OG_2 : Cathode-ray oscillograph
DR : Data recorder
H : Frequency analyzer
P : X-Y plotter

Fig.9 Experimental planetary gear train of power circulating type

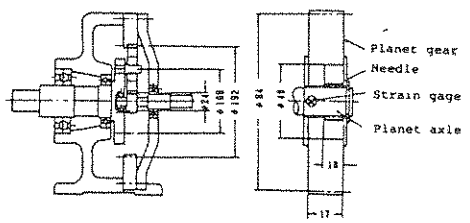

Sun gear : $Z_1=16$, $b_1=19$, SCM3 $i=1/9$
Planetary gear : $Z_2=56$, $b_2=17$, SCM21 $\alpha=20°$
Internal gear : $Z_3=128$, $b_3=19$, S45C $m=1.5$
Allowable tooth surface load :
$P_{max}=1\,230\,N(\kappa=35\,N/mm^2)$

Fig.10 Planetary gear

5.2 Tested planetary gears

A pair of planetary gears shown in Fig.10 with load balancing mechanism by means of the spring action of lubrication oil film in planet gear bearings are used. In the experiment a little grease is supplied to the planetary gears and the balancing mechanism does not work. The main errors in the planetary gears are the runout errors of the sun gear, the planet gears, the internal gear and relative tooth profile errors between the sun gear and the planet gears. The amplitude of each runout error are shown in Table 4 and the tooth profile errors and the transmission errors due to the profile errors are shown in Fig.11(a) and (b) respectively.

Table 4 Eccentricity error of each gear

Sun gear	planet gear			Internal gear
	1	2	3	
12.7	30	31	26	51.6

6. Experimental Measurement of Load Sharing

The experimental measurement was done under the driving conditions with combination of the rotational speed N [rpm] and the torque T [N·m] as shown in Table 5. As the lubricant a little grease was applied on the contact surface in the tested planetary gears. An example of the recorded electromagnetic oscillograms of load variation curves on every planet gear axis is shown in Fig.12. There, the rotational speed of sun gear is 600rpm. For all driving conditions the shapes of the curves are almost similar but the amplitudes are different. The total amplitudes and the mean amplitudes of the load variations on each planet gear axis for all driving conditions are read out and summarized in Fig.13, in which, the upper horizontal limit line shows the maximum load and its height shows the amplitude of the variation, the middle horizontal line shows the mean value of the load in each

Table 5 Operating conditions

Rotational speed N (rpm)	600	1200	2500	3500	5000	Testing maching maximum rotational speed 98000(rpm)

Load	Output T (N·m)	0	85.5	142.5	228	Limit load Pmax 1230(N)
	Tooth surface load P (N)	0	260	440	700	

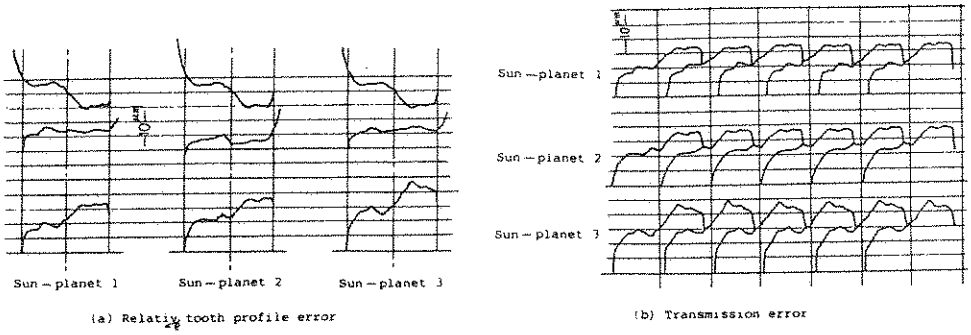

(a) Relative tooth profile error (b) Transmission error

Fig.11 Transmission error curve and relative tooth profile error between sun gear and planetary gear

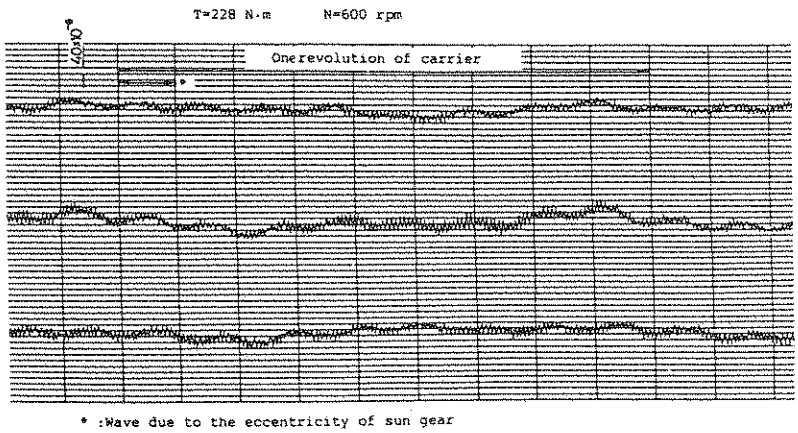

* :Wave due to the eccentricity of sun gear

Fig.12 Measured curve of load variation

histogram and the numbers 1, 2 and 3 indicate the planet gears. For example, the group in the right side of Fig.(a) shows that the amplitude of the load variation and the sharing load of the 3rd planet gear take the maximum value at the torque T=228N・m. From discussions about the values of load sharing factors of the mean load that are written in Fig.(a), the followings are concluded.

(1) The effect of the load : The load sharing conditions, when the rotational speed N is kept constant at 3500 rpm and the values of the load are changed, are shown in Fig.(a). It is seen that the amplitudes of the variations of the load on every planet axis is increased but the load sharing factors of mean loads come close to unity (improved) with an increasing load.

(2) The effect of the rotational speed : The load sharing conditions, when the torque T=228N・m constant and the rotational speeds are changed, are shown in Fig.(b). It is seen that with an increase of the rotational speed the amplitudes of the load variation are slightly increased but the values of the load sharing factor remain almost constant with an increase of the rotational speeds.

7. Considerations

7.1 The fundamental consideration on the relation between the gear errors and the load variations

The load variations in the planetary gears are caused by the errors in gears and the other parts and there are two types of the variations. Defining the transmission error on i-th planet gear train as e_i (the function of the rotational angle) and the mean value of e_i's as $\bar{e}$,

(1) $\bar{e}$ becomes the transmission error between the input and output shafts and excites the vibration system of the total mechanism and becomes the cause of the dynamic load P_d,

(2) $(\bar{e}-e_i)$ is the main factor to decide the values of load sharing factors and becomes the cause of uneven load on every planet gear. Because the load sharing factor ν_i is expressed by the following Eq.(8) (when there is no gap in every bearing) .

$$\nu_i=1-\frac{(\bar{e}-e_i)}{(C_0+1.5C_a)} \quad \cdots\cdots(8)$$

where, $(C_0+1.5C_a)$ is the equivalent tooth face error. The distinguished gear errors that are detected in the measurement of the tested planetary gears are the relative tooth profile error between the sun gear and planet gears and the runout errors of the sun gear, planet gears, internal gear and the carieer and the data on them are given in Table 6 with some needed data about the dynamic load P_d and the load sharing factors ν_i .

7.2 The observational study on load variation curves

It is seen that the cyclic error components due to the harmonics of every gear error are contained in the load variation curves of the experiments. The

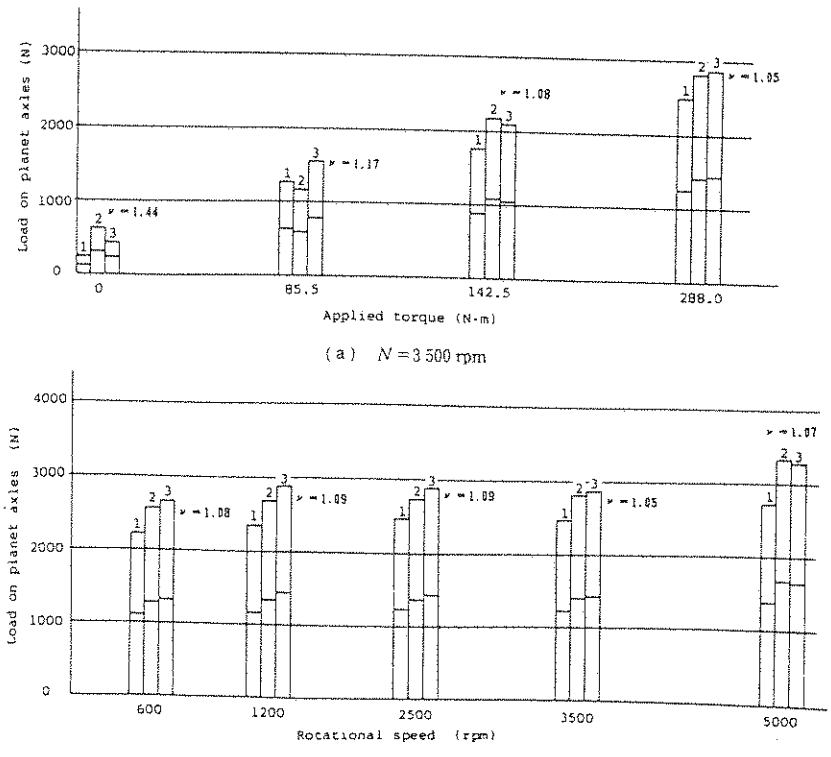

(a) $N=3500$ rpm

(b) $T=228$ N・m

Fig.13 Full amplitude of load variation

followings are seen (see Fig.12).

(1) An error component with a short period λ_1 that is due to the tooth profile error is seen and the load variation curves for each planet gear axis have the same phase in some parts and do not in the other parts. It must mean that every planet gear moves with very complicated motion.

(2) An error component with a secondary short period of λ_2 ($=16\cdot\lambda_1$) is seen. There are the phase shifts of about 1/3 of the period between the components of each axis. It seems that the error is due to the runout error of sun gear.

(3) An error with a period of λ_3 ($=3\sim4\cdot\lambda_2$) is seen in high speed drive. All curves have the same phase and the error is likely to be due to the runout error of the planet gears.

(4) An error with the longest period λ_4 ($=9$ times of λ_2), is seen but the cause is not made clear yet.

Table 6 Factors influencing on load variation

Sort of errors	Shape of errors	Effecfive factors to P_d $\bar{e}$	Effecfive factors to y_i $\bar{e}-e_i$	Ratios of periods	Wave lengths of errors
Sun planet tooth profile error e_{sp}	Total amplitude 10~14 μm saw tooth shape	2.3 μm	$\frac{e_{sp}}{\cos 20}$ =15 μm	1/16	λ_1
Eccentric error of sun gear e_s	Half amplitude 7 μm sinusoidal shape	0	$\frac{e_s}{\cos 20}$=7.4 μm	1	λ_2
Esentric error of planet gear e_{pi}	Half amplitude 13~16 μm sinusoidal shape	$2e_p$=29μm	3 μm	3.5	λ_3
Eccentric error of internal gear e_r	51.6 μm	0	$\frac{e_r}{\cos 20}$=54.9 μm	8	λ_4
Eccentric error of carrier e_c	30 μm		$2e_c$=60μm		

Table 7 Each component of bearing load of planetary gear

Wave lengths	Axles NO.	Rotational speed (rpm) 600	1200	2500	3500	5000
λ_1	1	3.7	4.8	41.9	18.4	59.9
	2	6.3	9.2	45.3	32.1	40.3
	3	4.8	6.2	42.8	37.2	53.5
λ_2	1	20.6	17.6	28.9	35.6	31.9
	2	7.7	18.9	28.2	66.5	43.7
	3	19.4	20.7	32.2	39.0	44.8
λ_3	1	72.4	50.0	52.7	25.9	50.5
	2	58.5	54.6	39.8	23.7	40.1
	3	77.1	59.7	41.3	32.0	39.0
λ_4	1	842.4	675.0	742.5	720.9	621.0
	2	938.1	776.5	815.2	774.2	617.1
	3	934.1	803.2	867.2	884.6	788.6

Table 8 Ratio of maximum load sharing ratio to mean amplitude of bearing load

Wave lengths	Rotational speed (rpm) 600	1200	2500	3500	5000
λ_1	1.28 / 4.9	1.37 / 6.7	1.05 / 43.3	1.27 / 29.2	1/17 / 51.2
λ_2	1.30 / 15.9	1.09 / 19.0	1.08 / 29.7	1.41 / 47.0	1.12 / 40.1
λ_3	1.11 / 69.3	1.09 / 54.8	1.18 / 44.6	1.18 / 27.2	1.17 / 43.2
λ_4	1.04 / 905.0	1.07 / 751.6	1.07 / 808.3	1.12 / 793.2	1.17 / 675.6

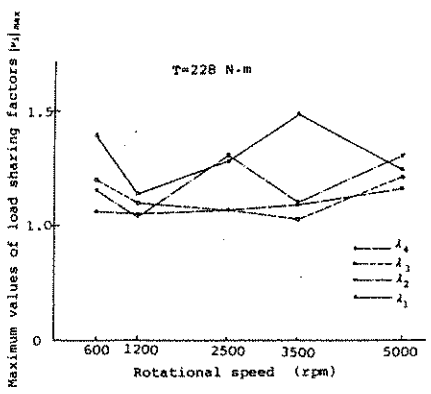

Fig.14 Comparison of load sharing ratio of each component

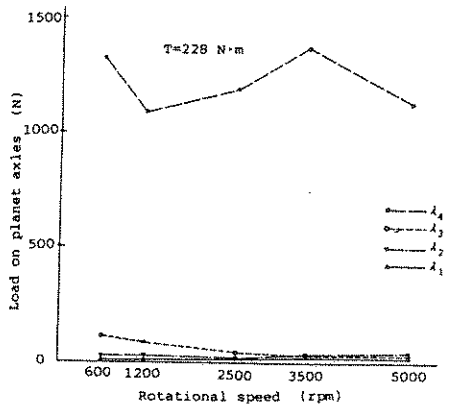

Fig.15 Mean load of each component

7.3 A quantitative consideration on the load sharing condition

Referring to the results of the observational consideration, a harmonic analysis of the variation curves has been done. The results, when the torque is constant (T=142.5N·m) and the rotational speed has 5 kinds of values, are shown in Table 7, where, the numerical values indicate the half amplitudes of λ_i components of the load on the planet gear axis 1, 2 and 3. The values of the maximum load sharing factor ν_{max} and the mean amplitudes 2·P(N) of loads of every planet gear axis obtained from Table 8 are shown in Table 7. The followings are known from the table.

(1) The values of the load sharing factors for λ_1 and λ_2 components vary with the rotational speed but there is not seen any regularity.

(2) The load sharing factors for λ_3 component ought to be unity because the value of $(e_i - \bar{e})$ is as small as 3 μm (see Table 6), but the factors change the value in low speed and have almost a constant value of about 1.18 when the rotational speed becomes more than 2500 rpm.

(3) The value of the factor for λ_4 component increases with the rotational speed.

The load sharing factors of every component of variation curves are compared in Fig.14, where,the values of factors for λ_1 and λ_2 components with short period change largely with the change of rotational speed but do not largely change for the components λ_3 and λ_4 . More study will be needed to clarify the reasons. Every harmonic component of the mean load of the 3 planet gear axes for each load conditions, the effects of the value of the load are very small for λ_1 , λ_2 and λ_3 components but large for λ_4 component (see Fig.15). The effect of the runout errors of the carieer is the biggest.

8. Conclusion

Summarizing the above, it can be concluded :

(1) An measuring method of the load of a planet gear axis by measuring the shearing strain of the axis is tested and it is confirmed that the method is available for practical use in all respects of the measuring error, the sensitivity and the simplicity of excution ; and

(2) through the experimental measurement of actual planetary gears, it has been made clear that the load sharing on each planet gear in dynamic condition is considerably different from the estimated one from the static condition.

A useful experimental method to prove the loaded condition in planetary gears could be obtained by this study. An analysis of the condition of the dynamic load in planetary gears condition is expected to be developed using the method.

References

(1) Report of the Developement Work on Steam Turbine Reduction Gears, Department of Ship, Ministry of Trasnportation (1970)
(2) T.HAYASHI, Load Balancing Theory in Planetary Gears, Journal of JSME, 36-288 (1970),1394
(3) JSME Handbook of Mechanical Engineering, The Fourth Edition, 4-43 (1965)